

# Mechanism Of Alpha Mangosteen As An Inhibitor Of Matrixmetalloproteinase-1 In Skin Cancer: *In-Silico* Study

Adryan Fristiohady<sup>1\*</sup>, Arfan Arfan<sup>1</sup>, Rathapon Asasutjarit<sup>2</sup>, Lidya Agriningsih Haruna<sup>2</sup>, La Ode Muhammad Julian Purnama<sup>2</sup>, Idin Sahidin<sup>1</sup>, Fadhliyah Malik<sup>1</sup>, Rezky Marwah Kirana<sup>1</sup>, Laode Kardin<sup>3</sup>, Loly Subhiaty Idrus<sup>1</sup>, Muhammad Hajrul Malaka<sup>1,2</sup>

<sup>1</sup>Faculty of Pharmacy, Universitas Halu Oleo, Kendari, Indonesia

<sup>2</sup>Faculty of Pharmacy, Thammasat University, Pathum Thani, Thailand

<sup>3</sup>Faculty of Medicine, Universitas Halu Oleo, Kendari, Indonesia Fakultas Farmasi, Universitas Halu Oleo

**Citation:** Fristiohady, A. (2024). Mechanism Of Alpha Mangosteen As An Inhibitor Of Matrixmetalloproteinase-1 In Skin Cancer: In-Silico Study. *Jurnal Mandala Pharmacon Indonesia*, 10(1), 218-226  
<https://doi.org/10.35311/jmpi.v10i1.505>

**Submitted:** 13 March 2024

**Accepted:** 06 June 2024

**Published:** 30 June 2024

\*Corresponding Author:  
**Adryan Fristiohady**  
Email:  
[adryanfristiohady@uho.ac.id](mailto:adryanfristiohady@uho.ac.id)



Jurnal Mandala Pharmacon Indonesia is licensed under a Creative Commons Attribution 4.0 International License

## ABSTRAK

Kanker kulit adalah salah satu keganasan yang paling umum menyerang banyak orang. Perkembangan kanker kulit disebabkan oleh paparan radiasi ultraviolet (UV) yang terputus-putus atau jangka panjang yang mengakibatkan berkurangnya respons imun yang diperantarai oleh sel, produksi spesies oksigen reaktif (ROS), dan perubahan DNA. Peningkatan kadar ROS dapat menginduksi produksi matrix metalloproteinases (MMPs).  $\alpha$ -mangostin ( $\alpha$ -MG) dari buah *Garcinia mangostana* Linn menunjukkan potensi sebagai agen anti-metastasis dengan mengurangi ekspresi MMP-1. Penelitian ini bertujuan untuk mengetahui afinitas dan profil stabilitas  $\alpha$ -MG sebagai anti kanker kulit dengan menerapkan metode in silico. Simulasi molekuler  $\alpha$ -MG berhasil diikatkan pada MMP-1.  $\alpha$ -MG menunjukkan hasil yang stabil setelah simulasi dinamika molekuler 100 ns berdasarkan *root mean square deviation* (RMSD) dan *root mean squared fluctuation* (RMSF). Energi pengikatan turunan xanton dihitung dengan menggunakan metode MM/PBSA.

**Kata Kunci:**  $\alpha$ -mangostin, MMP-1, Pendekatan in-silico

## ABSTRACT

Skin cancer is one of the most common malignancies affecting many people. The development of skin cancer is mainly due to intermittent or long-term exposure to ultraviolet (UV) radiation resulting in reduced cell-mediated immune response, production of reactive oxygen species (ROS), and DNA changes. Increased levels of ROS can induce the production of matrix metalloproteinases (MMPs).  $\alpha$ -mangostin ( $\alpha$ -MG) from fruit of *Garcinia mangostana* Linn pericarps showing potential as an anti-metastatic agent with reduced the expression of MMP-1. This study aims to determine the affinity and stability profiles of  $\alpha$ -MG as anti-skin cancer by applying the *in silico* method. Molecular simulation of  $\alpha$ -MG was successfully docked to the MMP-1.  $\alpha$ -MG showed stable results after 100 ns molecular dynamics simulation based on the root mean square deviation (RMSD) and the root mean squared fluctuation (RMSF). The binding energies of the xanthone derivatives were calculated using the MM/PBSA method.

**Keywords:**  $\alpha$ -mangostin, MMP-1, *in-silico approach*

## INTRODUCTION

$\alpha$ -mangostin ( $\alpha$ -MG) is a metabolite of 1,3,6,7-tetrahydroxy-2,8-di-(3-methyl-2-butenyl) xanthenes isolated from fruit of *Garcinia mangostana* Linn pericarps (78% content) (Meylina et al., 2021; Zhang et al., 2017).  $\alpha$ -MG has been reported to possess a variety of pharmacological properties, such as antioxidant, antiinfective, antidiabetic, neuroprotective, hepatoprotective, and

cardioprotective properties, and anticarcinogenic activity (Zhang et al., 2017). As well as anticancer properties in various kinds of cancers such as colon, lung, pancreas, breast, skin, and blood (Meylina et al., 2021).  $\alpha$ -MG works on all the major stages of tumor growth: initiation, promotion, and progression.  $\alpha$ -MG acts as a blocking agent by the modulation of enzymes involved in the metabolic activation and excretion of carcinogens, resistance to

oxidative damage, and attenuation of inflammatory response, while the inhibition of cell proliferation through modulating cell cycle regulatory machinery, induction of apoptotic effects on damaged and transformed cells, and blockage of angiogenic and metastatic processes of tumor cells contribute to its potential as a suppressing agent (Zhang et al., 2017; Ibrahim et al., 2016; Shan et al., 2011).

The  $\alpha$ -MG showing potential as an anti-metastatic agent with suppressed the metastatic processes of two Human Skin Cancer Cell Lines (SK-MEL-28 and A-431) (Wang et al., 2012). Treatment with  $\alpha$ -MG exhibited the greatest effects in reducing UVB-induced skin wrinkles, inhibited epidermal thickening, reduced the expression of MMP-1 and MMP-9 in hairless mice *in vivo*.  $\alpha$ -mangostin could suppress the UVB-induced phosphorylation of MAPKs, including ERK, p38 and JNK (Im et al., 2017).

Skin cancer is one of the most common malignancies affecting many people in many countries worldwide (Shadab et al., 2021). The development of skin cancer is mainly due to intermittent or long-term exposure to ultraviolet (UV) radiation resulting in reduced cell-mediated immune response, production of reactive oxygen species (ROS), and DNA changes (Asasutjarit et al., 2019). Increased levels of ROS can induce the production of matrix metalloproteinases (MMPs) (Shadab et al., 2021). It has been reported that MMP expression is increased in various cancers indicative of invasive disease and involves the motility of metastatic cells. Inhibiting cancer cell metastasis is one of the strategies for cancer therapy and research (Wu et al., 2016). Metastasis is a complex process involving adhesion, migration, and invasion (Ji et al., 2015).

Cancer invasion depends on the action of extracellularly secreted proteases such as MMPs (Wu et al., 2016). MMPs are classified according to their primary function, collagenase, gelatinase, stromelysins, and matrilysins. MMP-1 is a type of collagenase that correlates with increased invasion and metastasis in melanoma (Bastian et al., 2017). These MMPs are secreted from cancer cells to

degrade ECM proteins at the basement membrane barrier, promoting migration and invasion of cancer cells. Upregulated MMP-1 expression after UV irradiation resulted in collagen degradation.

The MMP-1 initiates the degradation of collagen types I and III and further degrades the collagen fragments produced by collagenase (Im et al., 2017). Therefore, suppression of MMP-1 is one strategy to prevent metastasis of cancer cells (Wu et al., 2016). Many previous studies has found the activity of  $\alpha$ -MG inhibits oncogenic marker, but there is no specific reported the inhibitory effect of  $\alpha$ -MG towards MMP-1 in skin cancer.

## RESEARCH METHODS

We selected the three-dimensional structure of human fibroblast collagenase-1, also known as matrix metalloprotease-1 (MMP-1), from Protein Data Bank (PDB ID: 966C) (<https://www.rcsb.org/>). MMP-1 was generated by eliminating water molecules, and then the polar hydrogen atoms and Kollman charge were added utilizing AutoDock Tool 1.5.6 (Morris et al., 2009).

### Ligand preparation

In this study, we focused on identifying the potential of xanthone derivatives ( $\alpha$ -MG) against MMP-1. The native ligand (RS2) and fluorouracil were used as control molecules because they are known to inhibit the MMP-1 activity. All the molecules were collected from the PubChem database (<https://pubchem.ncbi.nlm.nih.gov/>) and prepared by adding Gasteiger charge and set to rotate freely on the same program in protein preparation.

### Molecular Docking Simulation

The docking simulations were run with AutoDock Tool 1.5.6 (Morris et al., 2009). The redocking process of the native ligand to the MMP-1 is a way to validate the docking protocol. Proper protocols were presented with a root mean square deviation (RMSD) value below 2 Å. The binding sites are arranged according to the RS2 coordinates on the x, y, and z-axis. The grid area was set to 34 x 30 x34 Å

with 0.375 Å point spacing. The interactions of each molecule are visualized with the PoseView (Stierand et al., 2006). Integrated into the ProteinsPlus web service (<https://proteins.plus/>) (Schöning-Stierand et al., 2020) and Discovery Studio Visualizer v17.2.0.16349 software.

### Molecular Dynamics Simulation

The best conformation of the xanthone derivatives were continued to molecular dynamics simulation to monitor its stability with the help of GROMACS 2016 (Abraham et al., 2015). The simulation utilizes the AMBER99SB-ILDN force field (Petrov and Zagrovic, 2014), monitored for 100 ns. Parametric files of molecules were generated using ACPYPE (Sousa Da Silva & Vranken, 2012). The TIP3P water model was employed for the solvation process, which is set at 310 K and neutralized by adding Na and Cl ions. The electrostatic force mimics the Particle Mesh Ewald method. The stability of the complex during the simulation was determined by analyzing the root-mean-square deviation and fluctuations (RMSD and RMSF), Solvent accessible surface area (SASA), principal component analysis (PCA), and radius of gyration (Rg) parameters. The binding energies of the xanthone derivatives were also calculated by applying the MM/PBSA method in g\_mmpbsa package (Kumari et al., 2014).

## RESULTS AND DISCUSSION

The development of skin cancer is mainly caused by intermittent or long-term exposure to ultraviolet (UV) radiation, thereby reducing cell-mediated immune responses, production of ROS) and DNA changes (Asasutjarit et al., 2021). Increased levels of ROS can induce the production of MMPs (Shadab et al., 2021). It has been reported that MMP expression is increased in various types of cancer, which is indicative of an invasive disease and involves the motility of metastatic cells. Inhibiting cancer cell metastasis is one of the strategies for cancer therapy and research (Ganesh & Massagué, 2021; Wu et al., 2016)

Metastasis is a complex process involving adhesion, migration and invasion (Ji et al., 2015). Cancer invasion depends on the

action of extracellularly secreted proteases such as MMPs (Wu et al., 2016). MMPs are classified according to their main functions, collagenases, gelatinases, stromelysins, and matrilysins. MMP-1 is a type of collagenase that correlates with increased invasion and metastasis in melanoma (Bastian et al., 2017).

These MMPs are secreted from cancer cells to degrade ECM proteins at the basement membrane barrier which ultimately promote migration and invasion of cancer cells. Upregulated MMP-1 expression after UV irradiation resulted in collagen degradation. MMP-1 initiates the degradation of collagen types I and III and further degrades collagen fragments produced by collagenase (Im et al., 2017). Therefore, suppression of MMP-1 is one strategy to prevent cancer cell metastasis (Wu et al., 2016).

### Molecular docking

Our aim in docking native ligand (RS2) to the MMP-1 target was to validate the grid parameters before the xanthone derivatives were docked to the target protein. We use the RMSD criteria as a grid validation parameter with a recommended value of less than 2 Å. RS2 was chosen as a reference because it could bind and inhibit MMP-1 with an inhibition constant of 23 nM. Based on the results, the MMP-1 binding site has coordinates  $x = 9.166$ ,  $y = -10.353$ , and  $z = 38.398$ . These coordinates were chosen as the docking protocol because they fulfill the recommended criteria with an RMSD of 0.9017 Å (Figure 1a). RS2 has a binding affinity of -9.62 kcal/mol, interacting with the zinc atom's catalytic site and the essential amino acids Leu181 and Ala182 at the active site MMP-1 (Lovejoy et al., 1999).

Molecular docking of  $\alpha$ -MG showed that the compound had a slightly lower binding energy than the original ligand, which was -8.78 kcal/mol. In general, these xanthone derivatives exhibit binding modes and interactions in the form of hydrogen bonds on the hydroxy groups of the xanthone ring with the amino acids Leu181 and Asn180 (Figure 1b). Uniquely, hydrogen bonding at residue Arg214 only appears in  $\alpha$ -MG. Hydrophobic interactions of

xanthone rings of these three compounds formed hydrophobic interactions with the amino acids Leu181, His218, Pro238, and Tyr240.

As a control, fluorouracil had the lowest binding energy with -4.10 kcal/mol and formed

two hydrogen bonds with residues Tyr237 and Thr241 (Figure 1c). The amine and hydroxy groups in this compound play an essential role in binding to the active site of MMP-1.

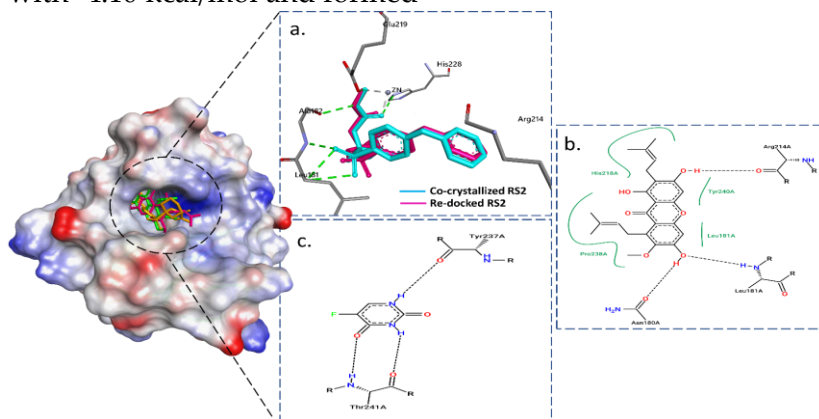


Figure 1. Molecular interactions of xanthone derivatives with MMP-1. (a) Overlay 3D conformation of co-crystallized and docked RS2. 2D interactions of (b)  $\alpha$ -MG, and (c) fluorouracil with MMP-1

Molecular docking has proven to be a successful tool for rapidly identifying functional compounds (Lin et al., 2020). We evaluated the structure of MMP-1 based on molecular docking and dynamics simulation to ascertain its inhibitory potential of xanthone analog as skin cancer drug candidates. It was observed that  $\alpha$ -MG could bind to the catalytic site of MMP-1.

This analog has a similar predictive affinity to the native ligand (RS2) as an MMP-1 inhibitor (Lovejoy et al., 1999). The docking study showed  $\alpha$ -MG interacted with catalytic residues such as Asn180, Leu181, Ala182, and Arg214. These residues are the most prominent pockets in the MMP catalytic domain

responsible for hydrogen bonding with the ligand.

### Molecular Dynamics Simulation

Mangostin analog was continued to predict its dynamic behavior towards MMP-1 for 100 ns through MD simulation. The stability and flexibility of the mangostin complex were analyzed based on RMSD and RMSF parameters and compared with RS2 and fluorouracil. The results can be seen in Figure 2, where all complexes have similar stability during the 100 ns simulation with complex fluctuations around 0.3 nm. The difference in mean flux was observed at RS2 complex, slightly lower with an RMSD value of 0.29 nm.

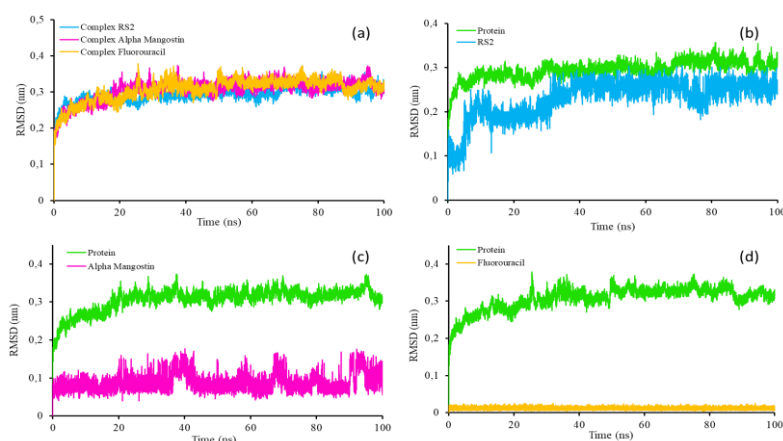


Figure 2. The RMSD plot of (a) backbone atoms for MMP-1 complex. The RMSD plot of protein and ligand for (b) RS2, (c)  $\alpha$ -MG, and (d) fluorouracil during 100 ns simulation



Ligand stability during the simulation was also observed during binding to MMP-1. In Figure 2b-d, it can be seen that fluorouracil is very stable as long as it is bound to MMP-1 with an RMSD ligand of 0.014 nm.  $\alpha$ -MG showed

better ligand stability than RS2, with an average RMSD ligand of 0.088 nm and 0.23 nm, respectively. This stable graphic pattern demonstrates the ability of  $\alpha$ -MG analogs to stabilize the complex during simulation.

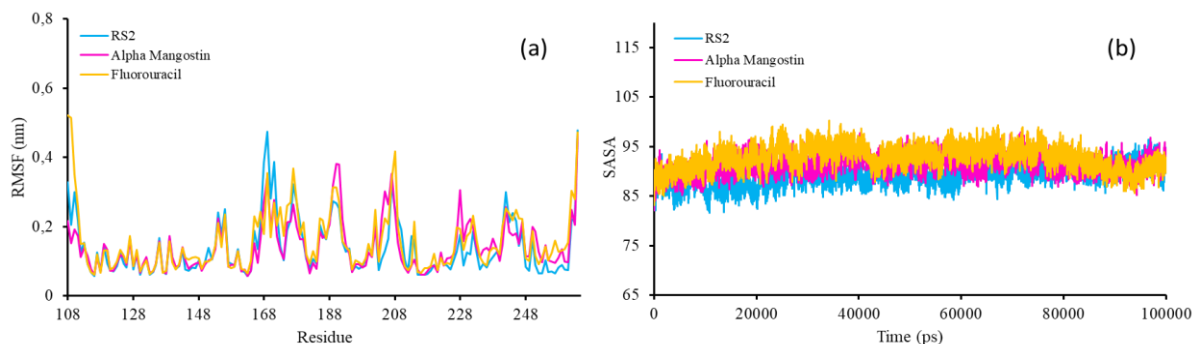


Figure 3. The Stability analysis (a) RMSF, and (b) SASA plots of backbone atoms for MMP-1 complex during 100 ns simulation

Analysis of amino acid oscillations in the MMP-1 backbone region showed various fluctuations at several residues (Figure 3a). The RMSF values were high at some residues, such as Arg169, and Arg208, at ~0.45 nm. Additionally, residues of Pro177, Ile191, His228, and Phe242 at ~0.3 nm. Arg108 and Gln264 residues of the complex in the MMP-1 loop region display high peak intensities with fluctuation values of ~0.5 nm. However, overall all complexes display similar fluctuation models during simulation.

Solvent Accessible Surface Area (SASA) analysis was performed on each complex to complete the stability analysis. Figure 3b displays the predicted areas on the receptor accessible to water molecules during the simulation. The smaller the site accessed by the water molecule, the more stable the ligand-receptor complex. The RS2 complex has an area accessible to the smallest water molecules with an area of 89.3 nm. The SASA area of  $\alpha$ -MG is 91.4 nm, and the widest is fluorouracil, with an area of 92.7 nm (Morris et al., 2009).

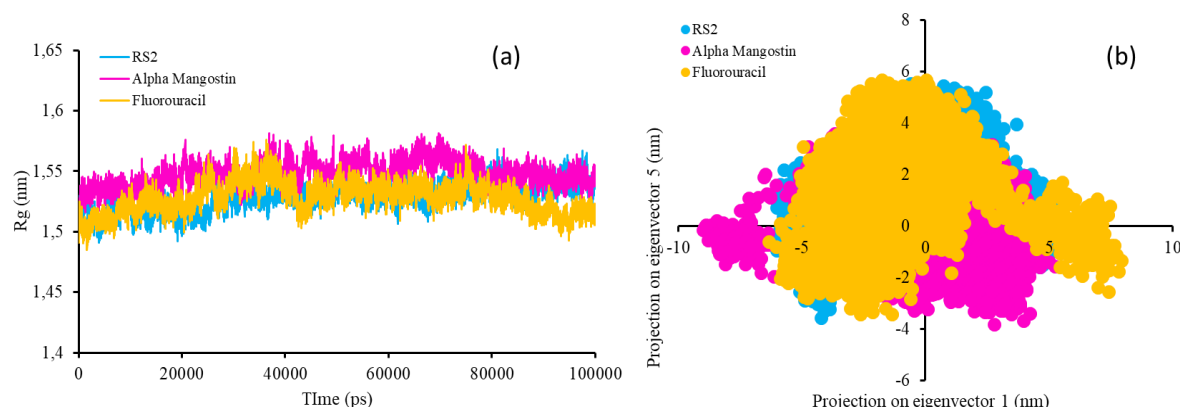


Figure 4. The Stability analysis (a) radius gyration, and (b) PCA of the trajectory in 2D plots of MMP-1 complex during 100 ns simulation

Radius gyration measurements were performed to assess receptor compactness during simulation (Figure 4a). The low and constant value of Rg during the simulation indicates a stable form of protein folding. It can be seen in the graph that all complexes have the same compactness from the beginning to the

end of the simulation, with an average Rg value of 1.52 nm.

The results showed that the  $\alpha$ -MG complex had increased the Rg value at a simulation time of ~70 ns to 1.55 nm. However, it decreases to be similar to RS2 at the end of the simulation, with a value of 1.52 nm. This result

also shows that the fluorouracil complex has the best compactness compared to other compounds at the end of the simulation, with an Rg value of 1.5 nm.

The basic dynamics patterns of all residues of the MMP-1 complex were identified and analyzed using principal component analysis. Most of the protein fluctuations can be explained by low and high projections on the eigenvectors. The motion of the backbone atoms

is captured in these two eigenvectors and visualized on a 2D Cartesian graph (Figure 4b).

The stable MMP-1 complex can be identified from the less space occupied by the cluster during the simulation. In 2D eigenvector plots, the RS2 complex was found to occupy less space than the other complexes. The  $\alpha$ -MG and fluorouracil complexes, showing the vector areas tend to be similar but in a different area.

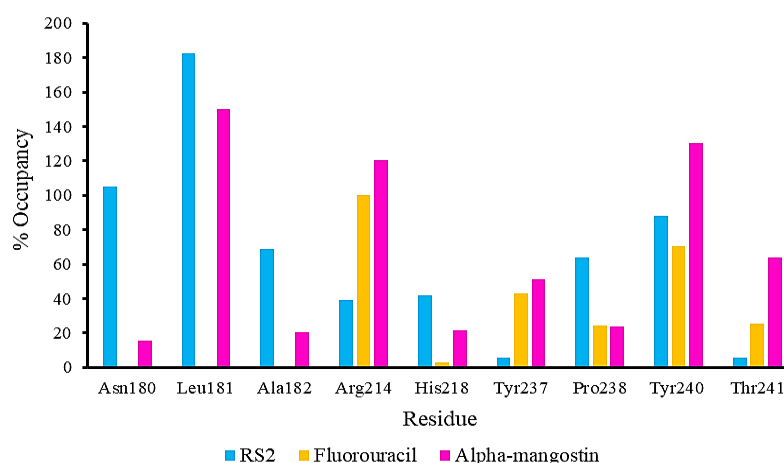


Figure 5. Percent occupancy of hydrogen bonds formed by the MMP-1 complex during the 100 ns simulation

Hydrogen bond occupancy was analyzed to determine the number and percentage of bonds formed from the complex during dynamic simulation (Figure 5). High H-bond occupancy (>100%) was observed in several residues, including Asn180, Leu181, Arg214, and Tyr240. The residue is part of the MMP-1 active site and was previously confirmed to be present in the docking process.

The native ligand (RS2) had the highest occupation of Leu181 residues with 182%, followed by  $\alpha$ -MG at 150%. Meanwhile, fluorouracil did not form hydrogen bonds with these residues during the simulation. Interestingly,  $\alpha$ -MG retains its hydrogen bonds with Arg214 with the highest occupancy at 120%, followed by fluorouracil at 100%. In contrast to RS2, which has the lowest occupancy of this residue with a value of 39%. Uniquely, hydrogen bonding with Tyr240 was not observed in the docking process. However, this residue showed relatively high H-bond occupancy in all complexes during the MD simulation with 130%, 88%, and 70.5% for  $\alpha$ -MG, RS2, and fluorouracil, respectively.

### Binding energy calculations

This research analyzes the binding energy with the MM-PBSA approach to compare the affinity of each compound against MMP-1. Several energies that affect to the binding affinity are examined, including Van der Waals ( $\Delta E_{VDW}$ ), electrostatic ( $\Delta E_{Ele}$ ), polar solvation ( $\Delta E_{PB}$ ), and SASA energy ( $\Delta E_{SASA}$ ). All these energies are calculated in kJ/mol (Table 1).

$\alpha$ -MG was predicted to have lower binding energies ( $\Delta E_{Bind}$ ) than RS2 (-83.73 kJ/mol) and fluorouracil (-37.12 KJ/mol).  $\alpha$ -MG has the most substantial binding energy with a value -119.85 kJ/mol. These results are suitable with predictions based on RMSD, RMSF, and Rg analysis complexes which revealed that  $\alpha$ -MG are more stable than the other compounds. These results demonstrate the ability of the analog mangostin to inhibit the MMP-1. The analysis showed that the Van der Waal and electrostatic energy had the most significant contribution to the binding affinity. Meanwhile, polar solvation energy is less favorable for complex systems.

Table 1. Binding energy prediction by the MM-PBSA method

No.	Compounds	$\Delta E_{VDW}$	$\Delta E_{Ele}$	$\Delta E_{PB}$	$\Delta E_{SASA}$	$\Delta E_{Bind}$
1	RS2	-156.62 $\pm$ 14.86	-23.69 $\pm$ 20.20	111.18 $\pm$ 28.89	-14.60 $\pm$ 1.22	-83.73 $\pm$ 24.80
2	Fluorouracil	-87.32 $\pm$ 7.33	-33.09 $\pm$ 14.38	91.05 $\pm$ 11.32	-7.74 $\pm$ 0.46	-37.12 $\pm$ 13.02
3	$\alpha$ -MG	-202.89 $\pm$ 14.33	-14.41 $\pm$ 10.5	116.26 $\pm$ 15.79	-18.8 $\pm$ 1.17	-119.85 $\pm$ 14.51

Dynamics simulations of the complex were conducted to evaluate the binding affinity, stability, and flexibility of mangostin analogs to MMP-1. We observed that the binding pattern obtained after MD simulation was very stable with an RMSD value of about 0.3 nm for all complexes. The effect of protein movement during the MD simulation can be observed from fluctuations in amino acids. The highest intensity fluctuations were seen in the Pro177, His228 and Phe 242 at the backbone and Gln265 at the C-terminal region.  $\alpha$ -MG showed stable conformational changes based on RMSD, RMSF, and Rg analysis.

This result is also supported by an analysis of binding energy with MM-PBSA and hydrogen bond occupancy, which shows the potential of  $\alpha$ -MG in binding and inhibiting MMP-1. Hydrogen bonding is one factor that plays a vital role in the binding process between ligands and receptors. Expression of MMP-1 by stromal fibroblasts causes connective tissue damage and increases skin cancer metastasis so that MMP-1 inhibition can reduce the severity of skin cancer (Zhang et al., 2017).

## CONCLUSION

This study was successfully docked  $\alpha$ -MG to the MMP-1 which is have anti-skin cancer activity.  $\alpha$ -MG compounds can inhibit MMP-1 based on the results of molecular docking and molecular dynamics simulations compared to fluorouracil. This research can be investigated further to prove the anti-skin cancer activity of the  $\alpha$ -MG compound through *in vitro* and *in vivo* tests.

## ACKNOWLEDGEMENTS

A.F and R.A would like to thank to Thammasat Postdoctoral 2021.

## REFERENCES

- Abdullah MZ, Bakar LM, Othman N, Taher M, Rasad MSBA, Foong FHN, Ichwan SJA. Anti-cancer Activities of  $\beta$ -mangostin Against Oral Squamous Cell Carcinoma. 2022. Journal of International Dental and Medical Research. 15(1):81-87. <http://www.jidmr.com>
- Abraham, M. J., Murtola, T., Schulz, R., Páll, S., Smith, J. C., Hess, B., & Lindah, E. (2015). Gromacs: High performance molecular simulations through multi-level parallelism from laptops to supercomputers. *SoftwareX*, 1–2, 19–25. <https://doi.org/10.1016/j.softx.2015.06.001>
- Asasutjarit, R., Meesomboon, T., Adulheem, P., Kittiwisut, S., Sookdee, P., Samosornsuk, W., & Fuongfuchai, A. (2019). Physicochemical properties of alpha-mangostin loaded nanomeulsions prepared by ultrasonication technique. *Heliyon*, 5(9), e02465. <https://doi.org/10.1016/j.heliyon.2019.e02465>
- Asasutjarit, R., Sooksai, N., Fristiohady, A., Lairungruang, K., Ng, S. F., & Fuongfuchai, A. (2021). Optimization of production parameters for andrographolide-loaded nanoemulsion preparation by microfluidization and evaluations of its bioactivities in skin cancer cells and uvb radiation-exposed skin. *Pharmaceutics*, 13(8). <https://doi.org/10.3390/pharmaceutics13081290>
- Bastian A, Nichita L, Zurac S. Matrix Metalloproteinases in Melanoma with and without Regression. 2017. The Role of Matrix Metalloproteinase in Human Body Pathologies. London: IntechOpen; 145. 10.5772/intechopen.72931

- Ganesh K, Massagué J. 2021. Targeting metastatic cancer. *Nat Med.* Jan;27(1):34-44. doi: 10.1038/s41591-020-01195-4.
- Ji BC, Hsiao YP, Tsai CH, Chang SJ, Hsu SC, Liu HC, Chung JG. Cantharidin impairs cell migration and invasion of A375. 2015. S2 human melanoma cells by suppressing MMP-2 and -9 through PI3K/NF- $\kappa$ B signaling pathways. *Anticancer research.* 35(2): 729-738.
- Im, A. R., Kim, Y. M., Chin, Y. W., & Chae, S. (2017). Protective effects of compounds from *Garcinia mangostana* L. (mangosteen) against UVB damage in HaCaT cells and hairless mice. *International Journal of Molecular Medicine*, 40(6), 1941–1949. <https://doi.org/10.3892/ijmm.2017.3188>
- Lovejoy B, Welch AR, Carr S, Luong C, Broka C, Hendricks R, Browner MF. 1999. Crystal structures of MMP-1 and -13 reveal the structural basis for selectivity of collagenase inhibitors. *Nature structural biology.* 6(3): 217-221. 10.1038/6657
- Kumari, R., Kumar, R., & Lynn, A. (2014). G-mmpbsa -A GROMACS tool for high-throughput MM-PBSA calculations. *Journal of Chemical Information and Modeling*, 54(7), 1951–1962. <https://doi.org/10.1021/ci500020m>
- Lin, X., Li, X., & Lin, X. (2020). A review on applications of computational methods in drug screening and design. *Molecules*, 25(6), 1–17. <https://doi.org/10.3390/molecules25061375>
- Meylina, L., Muchtaridi, M., Joni, I. M., Mohammed, A. F. A., & Wathoni, N. (2021). Nanoformulations of  $\alpha$ -mangostin for cancer drug delivery system. *Pharmaceutics*, 13(12). <https://doi.org/10.3390/pharmaceutics13121993>
- Morris GM, Huey R, Lindstrom W, Sanner MF, Belew RK, Goodsell DS, Olson AJ. 2009. AutoDock4 and AutoDockTools4: Automated docking with selective receptor flexibility. *Journal of computational chemistry.* 30(16), 2785–2791. <https://doi.org/10.1002/jcc.21256>
- Petrov D, Zagrovic B. 2014. Are current atomistic force fields accurate enough to study proteins in crowded environments?. *PLoS Computational Biology.* 10(5):e1003638. <https://doi.org/10.1371/journal.pcbi.1003638>
- Schöning-Stierand K, Diedrich K, Ehrt C, Flachsenberg F, Graef J, Sieg J, Penner P, Poppinga M, Ungethüm A, Rarey M. 2022. ProteinsPlus: a comprehensive collection of web-based molecular modeling tools. *Nucleic acids research.* 50(W1): W611–W615. <https://doi.org/10.1093/nar/gkac305>
- Shadab NA, Alhakamy T, Neamatallah S, Alshehri A, Mujtaba Y, Riadi AK, Radhakrishnan H, Khalilullah M, Gupta H, Akhter. 2021. Development, Characterization, and Evaluation of  $\alpha$  -Mangostin-Loaded Polymeric Nanoparticle Gel for Topical Therapy in Skin Cancer.
- Shan, T., Ma, Q., Guo, K., Liu, J., Li, W., Wang, F., & Wu, E. (2011). Xanthones from Mangosteen Extracts as Natural Chemopreventive Agents: Potential Anticancer Drugs. *Current Molecular Medicine*, 11(8), 666–677. <https://doi.org/10.2174/156652411797536679>
- Sousa Da Silva, A. W., & Vranken, W. F. (2012). ACPYPE - AnteChamber PYthon Parser interfacE. *BMC Research Notes*, 5, 1–8. <https://doi.org/10.1186/1756-0500-5-367>
- Stierand, K., Maaß, P. C., & Rarey, M. (2006). Molecular complexes at a glance: Automated generation of two-dimensional complex diagrams. *Bioinformatics*, 22(14), 1710–1716. <https://doi.org/10.1093/bioinformatics/btl>



150

- Wang, J. J., Sanderson, B. J. S., & Zhang, W. (2012). Significant anti-invasive activities of  $\alpha$ -mangostin from the mangosteen pericarp on two human skin cancer cell lines. *Anticancer Research*, 32(9), 3805–3816.
- Wu, Z. Y., Lien, J. C., Huang, Y. P., Liao, C. L., Lin, J. J., Fan, M. J., Ko, Y. C., Hsiao, Y. P., Lu, H. F., & Chung, J. G. (2016). Casticin inhibits A375.S2 human melanoma cell migration/invasion through downregulating NF- $\kappa$ B and matrix metalloproteinase-2 and -1. *Molecules*, 21(3). <https://doi.org/10.3390/molecules21030384>
- Zhang, K. J., Gu, Q. L., Yang, K., Ming, X. J., & Wang, J. X. (2017). Anticarcinogenic Effects of  $\alpha$ -Mangostin: A Review. *Planta Medica*, 83(3–4), 188–202. <https://doi.org/10.1055/s-0042-119651>